Presented at the 4th Joint Meeting of the US Sections of the Combustion Institute, Philadelphia, PA, March 20-23, 2005

The role of diffusion at shear layers in irregular detonations

Marco Arienti[1] Joseph E. Shepherd[2*]

[1]United Technologies Research Center, 411 Silver Lane, East Hartford, CT 06108
[2]California Institute of Technology, 1200 E. California Blvd., Pasadena, CA 91125

Abstract

We propose two simple models for evaluating the role of diffusion in the shear layer behind the triple point in the decaying portion of a detonation cell. Both models are based on an idealized detonation cell cycle, with imposed detonation speed profile. Following the standard triple-point analysis at the shock front, time-accurate integration of the species evolution is carried out using a detailed reaction mechanism and simplified models of mixing. The first model examined considers fast mixing of the fluid across the shear layer behind the triple point to map ignition enhancement as a function of mixture fraction. The second model is to treat the mixing layer as a one-dimensional, temporally-developing diffusion layer. Both model and simulations show that the effect of diffusion at the shear layer in the decaying portion of a detonation cell depends, as expected, on the activation energy of the reacting mixture. Negligible for regular detonation parameters, diffusion is found to significantly shorten the colder layer ignition delay in high-activation energy mixtures. Laminar flames are observed to emerge from the temporally developing shear layer in some cases.

1 Introduction

The standard detonation reaction structure, where convection balances chemical reaction, can be justified by asymptotic analysis (Clarke, 1983, 1989) and numerical studies (Singh *et al.*, 2003), which show that molecular and thermal transport effects can be neglected in one-dimensional detonation waves. In reality, detonation propagation is intrinsically three-dimensional with waves moving transversely to the main front. The resulting triple-points at the wave front create shear layers where thermal and mass diffusion may play a role.

The present work is motivated by Schlieren and PLIF images of shock configurations and OH reaction front structures in highly irregular fuel-oxidizer mixtures (Austin *et al.*, 2004). Contrary to the smooth flow features of regular detonations (Pintgen *et al.*, 2003), reaction fronts and shear layers in these images are highly wrinkled, with disorganized features suggesting that velocity and density fluctuations occur on a scale much smaller than the dominant cell width. With the appearance of these features, it is possible that diffusion can compete with convection as a transport mechanism and augment ignition and combustion. This is particularly relevant to to the propagation of irregular detonations because of the highly nonlinear coupling between fluid dynamics and chemical processes due to the high value of the effective activation energy, see Ul'yanitskii (1981). In irregular mixtures, temperature fluctuations of shocked fluid particles are strongly amplified by the chemical reactions, resulting in ignition delays that can provide a window of opportunity for diffusion effects to compete with convective adiabatic processes.

In this study, we suggest two very simple approaches to evaluate how diffusive molecular transport of radicals and energy could play a significant role in the combustion mechanism of detonations. In the first part of this paper, we propose a zero-dimensional model for bounding the possible role of diffusion in the decaying portion of a detonation cell; in the second part, we examine a more realistic one-dimensional model. Both models are solved numerically using detailed reaction networks with realistic rate constants and thermophysical properties.

*This work was carried out at the Caltech ASC Center for Simulation of Dynamic Response of Materials and funded by Contract B341492 under DOE Contract W-7405-ENG-48.

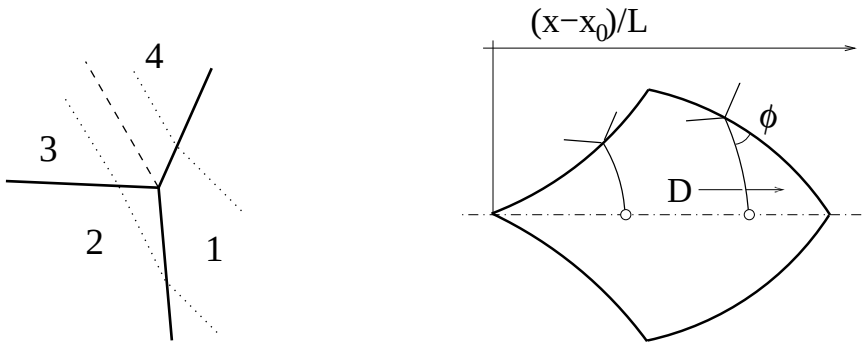

(a) (b)

Figure 1: Frame (a): Three-shock structure. Solid lines separate the undisturbed state (1) from the shock-compressed state behind the incident shock (2), the reflected shock (3), and the Mach stem (4). The dashed line represents the shear layer, and the two dotted lines are examples of particle paths. Frame (b): Idealized cell shape as described by two triple-point trajectories (thicker solid lines) symmetric with respect to the dash-dotted line. Also shown is a representative three-shock structure (thinner solid lines) at two distinct locations.

2 Homogeneous Mixing Ignition Model

Consider the simplest picture of regular cellular structure (Figure 1a), where a shear layer separates fluid particles that are compressed by the Mach stem (to state 4) from fluid particles that are compressed first by the incident shock (to state 2) and then by the reflected shock (to state 3). We will refer to these compressed states as the "hot" and "cold" streams, respectively, keeping in mind that the label "cold" may indicate temperatures that are much greater than the initial temperature T_1.

Our analysis is based on time-accurate constant-volume explosion calculations of shock-compressed fluid particles directly downstream of the triple point. When applied to regular detonation cells, this approach has lead to successful prediction of the keystone region shape of OH concentration Pintgen *et al.* (2003). The three-shock structure is computed using perfect-gas shock-polar analysis and the idealized detonation cell model of Figure 1(b). The calculation is simplified by assuming a constant angle ϕ between the triple point trajectory and the incident shock, and by neglecting shock curvature.

To bound the effect of diffusion on ignition, we assume first that the mixing between the two streams is infinitely fast. This is the homogeneous mixing ignition model (HMI) introduced by Knikker *et al.* (2003). The composition of the mixed material is defined by the mixture fraction Z of the cold stream and $(1-Z)$ of the hot stream. The mixture enthalpy is $h_m = Z h_{cold} + (1-Z)\, h_{hot}$ and the mixture composition (mass fraction) is $\mathbf{Y}_m = Z\mathbf{Y}_{cold} + (1-Z)\,\mathbf{Y}_{hot}$. Figure 2 shows the results of calculations carried out for a detonation in C_2H_4-$3O_2$-$8N_2$. Post-shock temperatures T_3 and T_4 (and pressure $P_3 = P_4$) define the initial conditions of the cold and hot gas. The temperature history is calculated with standard gas-phase chemistry models Kee *et al.* (1987, 1989) and a numerical solution (Shepherd, 1986) to either the constant-pressure or constant-volume explosion model.

In Figure 2(a), computed temperature histories are shown for for Z =0 (hot stream only), Z =0.50, 0.80, 0.95, and 0.99, showing that even a small amount of mixing can drastically reduce the time to ignition of the mixture. We define the adiabatic induction time τ^{cv} as the time necessary to reach 90% of the particle's peak temperature in constant-volume combustion. In Figure 2(a), the hot stream reacts after an induction time of less 5 μs, whereas the cold stream reacts much later, after 100 μs (with the GRI-Mech 3.0 mechanism by Smith *et al.*, 1995). Similarly to τ^{cv}, we define τ^{HMI} as the time necessary for the temperature to rise to 90% of the peak value in constant pressure combustion.

The mixture examined in Fig. 2, classified as strongly unstable (Austin, 2003), exhibits large lead shock oscillations, and front-reaction zone decoupling in the terminal portion of the detonation cell. The normalized activation energy is $\theta = E_a/RT_{vN}$ =12.4, where R is the universal gas constant and T_{vN} the von Neumann (post-shock) temperature. Shock polar analysis is carried out with track angle $\phi = 33°$ at a point located at 60% of the cell length. The resulting temperatures are $T_3 = 1276$ K and $T_4 = 1535$ K; the pressure is 6.561 atm.

Figure 2(b) shows the ignition times, τ^{cv}_{hot} and τ^{cv}_{cold}, computed by assuming a linear decrease of detonation speed from $1.4\,D_{CJ}$, at the beginning of the cell, to $0.7\,D_{CJ}$ at the end. Superimposed on the plot are the values of

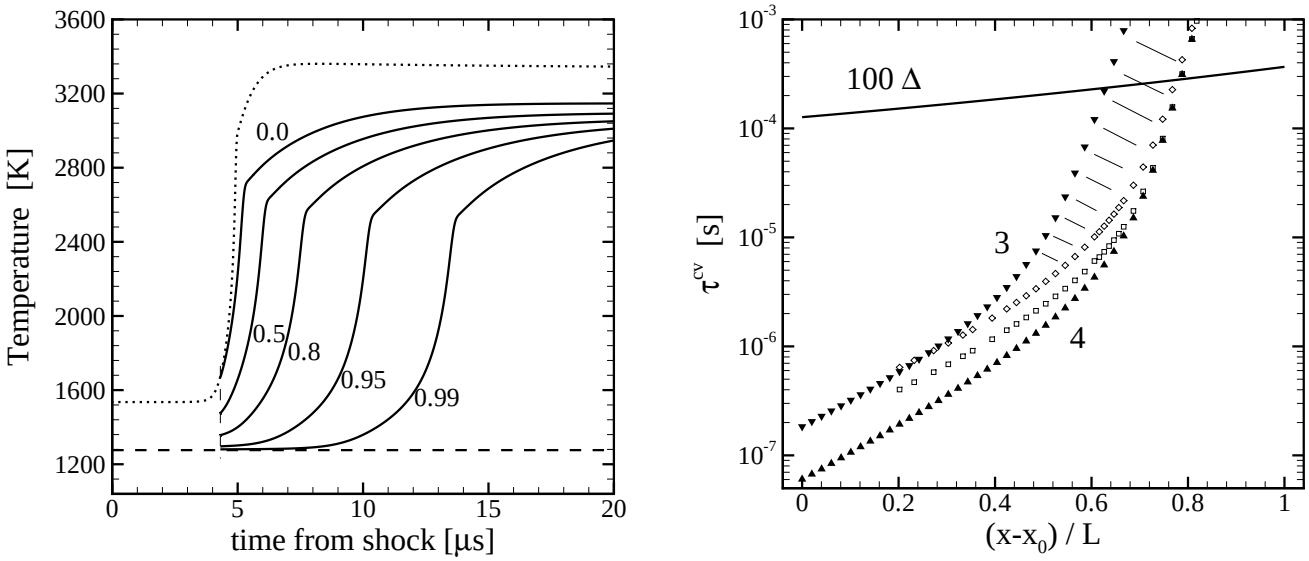

Figure 2: (a) Constant volume combustion of hot and cold stream (dotted and dashed lines respectively), and constant pressure combustion of four different hot stream-cold stream mixtures from $Z = 0$ (only hot stream), to $Z = 0.50$, 0.80, 0.95, and 0.99 for C_2H_4-$3O_2$-$8N_2$ ($P_1 = 6.67$ kPa and $T_1 = 298$ K). (b) Fast flame and diffusion flame ignition times as a function of non-dimensional distance from the cell apex for the same mixture. Constant volume adiabatic ignition time from post-shock state 3 (▼ symbol) and 4 (▲ symbol); constant pressure adiabatic ignition time from homogeneous mixing at $Z = 0.50$ (□ symbol) and $Z = 0.95$ (◊ symbol).

$\tau^{HMI}(0.5)$ and $\tau^{HMI}(0.95)$, evaluated by assuming constant-pressure combustion after a delay $\tau^{cv}_{hot}/10$ after the shock passage. The shaded area in the diagram shows the region where $\tau^{cv}_{cold} > \tau^{HMI}_{Z=0.95}$. Its width is almost one decade in time in the decaying half of our idealized cellular structure, showing that very modest amounts of mixing can accelerate the cold stream ignition by a factor of 10. This result reflects the high effective activation energy of the mixture under consideration. Similar calculations for regular mixtures (for instance, $2H_2 - O_2 - 7Ar$, not shown here), yield τ^{HMI} curves that are all very close to the τ^{cv}_{cold} curve.

Also shown in Figure 2(b) is the time $\tau^{100\Delta}$ necessary for a particle traveling at the post-shock particle speed u_3 to cover 100 times the induction length of the reference CJ-ZND profile, Δ. This arbitrary multiple of Δ is a reference time scale for "effective" energy release by the reactants, which has to occur within one cell length scale (approximately 200-300 times Δ) to push ahead the lead shock.

The large time scale separation between τ^{cv}_{cold} and τ^{cv}_{hot} suggests that molecular transport and thermal diffusion mechanisms can play a role in shortening the mixture ignition time in the decaying portion of a detonation cell. Figure 2(b) shows a ratio $\tau^{cv}_{cold}/\tau^{cv}_{hot} \approx 100$ at 60% of the cell length. After the 80% point, $\tau^{cv}_{cold} > \tau^{cv}_{hot} > \tau^{100\Delta}$, implying that adiabatic shock compression is not an effective mechanism for ignition.

3 One-Dimensional Model

The time scale estimates described in the previous section ignore the finite time required by diffusion to take place across the shear layer. A slightly more realistic model is to assume that the shear layer is temporally developing but spatially uniform, ignoring the relative velocity of the two streams but including species and temperature differences. This reduces the problem to a one-dimensional calculation that can be handled by methods developed for transient laminar flames. To carry out these calculations, a second-order reactive Riemann solver developed by Deiterding (2003) is augmented to include the effect of diffusion due to molecular transport with an operator splitting approach where each integration step is computed as a sequence of convection, diffusion, and constant-volume combustion sub-steps.

These computations include realistic transport mechanisms and rates. Species molecular transport is modeled

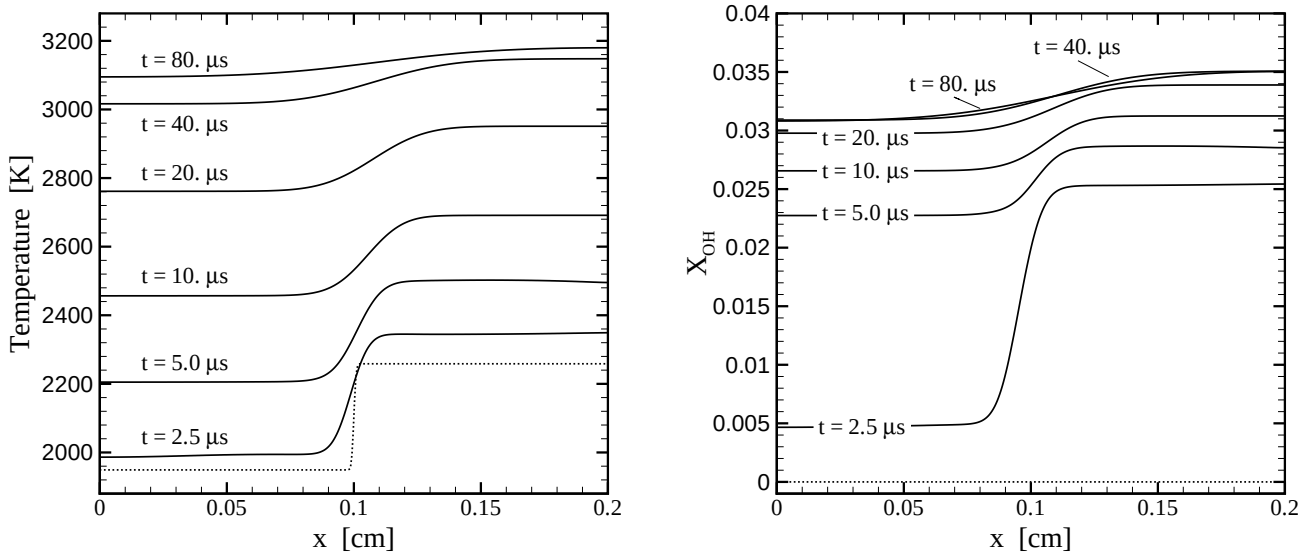

Figure 3: Temperature and OH concentration profiles for a one-dimensional diffusion layer simulating ignition across the mixing layer behind a triple point on an $2H_2$-O_2-7Ar detonation front. Time is measured from the point of shock passage (dotted line: initial conditions).

according to Fick's law, with diffusion velocities calculated from the species binary diffusion coefficients (Kee *et al.*, 1986, 2003). A correction velocity equal for all species is added to the convection velocity to ensure species mass conservation. This implementation corresponds to the best first-order approximation of the exact diffusion problem (Giovangigli, 1991).

Figure 3 shows temperature and OH concentration profiles computed for a $2H_2$-O_2-7Ar mixture at 0.1990 atm with the Miller & Bowman (1989) mechanism (also used in the following calculations). The initial conditions (dotted line) mimic the discontinuity at the shear layer immediately after the passage of the lead shock. The initial width of the interface, $d = 0.02$ mm, extends for 4 grid points (this rather coarse initialization was found not to affect the results). At $t = 0$, the hot and cold sides have same composition and pressure, with $T_{hot} = 2258$ K and $T_{cold} = 1949$ K. The constant-volume ignition times are $\tau^{cv}_{hot} = 0.92$ μs and $\tau^{cv}_{cold} = 1.6$ μs, with τ^{HMI} not appreciably smaller than τ^{cv}_{cold}. The simulation shows that the effect of diffusion on induction time is negligible for regular detonations.

Our next simulation is carried out for $2H_2$-O_2-$8N_2$ at 3.352 atm. Compared to the argon-diluted case, this mixture has a larger normalized activation energy (between 7.8 and 8.3, depending on the reaction model), and can be classified as moderately to highly unstable. This larger sensitivity to flow conditions makes a meaningful separation of convective and diffusive effects more difficult. It is instructive to consider the situation where the hot stream has already reached its equilibrium composition after reaction while still being a reservoir of high-temperature products and radicals. In Figure 4, time is measured after the complete burn of the hot fluid particle. At $t = 0$, $T_{hot} = 2213$ K and $T_{cold} = 1020$ K (dotted line). At the condition specified for the cold layer, adiabatic ignition would take place after $\tau^{cv}_{cold} = 1470$ μs. By including the effect of molecular and heat transport, a temperature bulge appears in the first 47.5 μs, followed by a fully developed laminar diffusion flame that steadily propagates toward the cold layer. This result favorably compares with the estimate $\tau^{HMI}(0.95) = 17$ μs from our zero-dimensional model.

We conclude with an example that separates the effect of OH radicals diffusion from the effect of thermal diffusion only. Figure 5 shows the results of two calculations for the same initial conditions described above: the reference case of premixed $2H_2$-O_2-$11N_2$, with $\tau^{HMI}(0.95) = 162$ μs; and the case where the hot layer is substituted by inert N_2 at the same temperature (dashed line). In the case where no radicals are initially available, the laminar diffusion flame takes approximately 100 μs more to develop. Similar calculations of other cases show, however, much less sensitivity to the radical concentration.

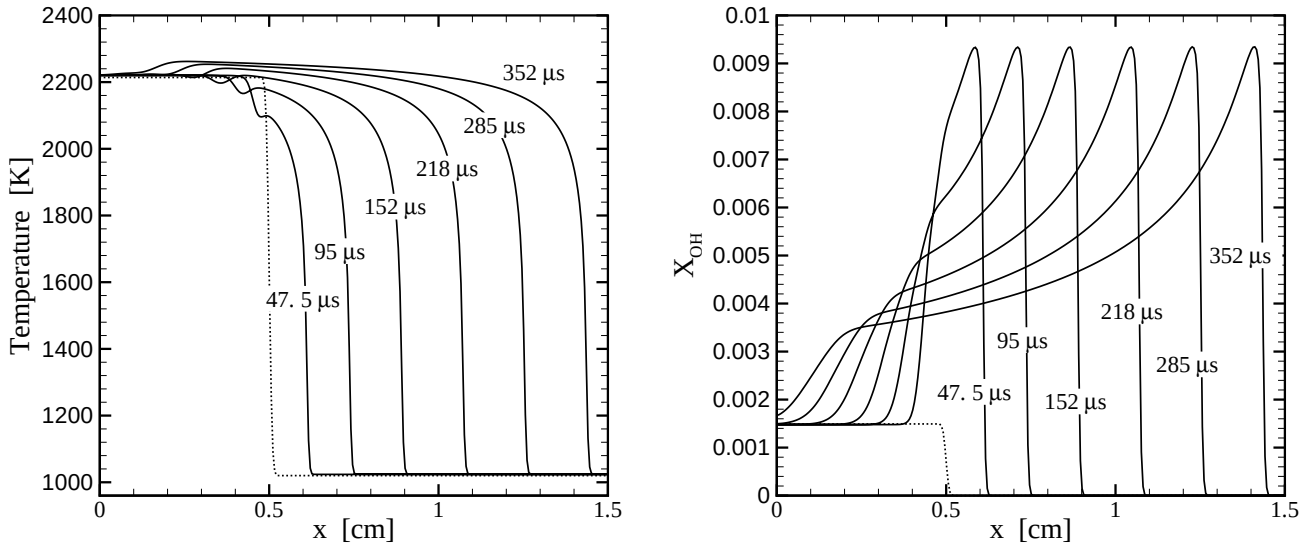

(a) (b)

Figure 4: Temperature and OH concentration for temporal development of a diffusion layer in $2H_2$-O_2-$8N_2$. Time is measured after the complete burn of the hot layer (dotted line: initial conditions after the hot stream has reached its equilibrium composition).

4 Conclusions

The intrinsic large separation of ignition time scales in irregular detonations has been examined here as a window of opportunity for diffusion to compete with convective adiabatic processes. We have focused our attention to the shear layer region behind the triple points on the lead shock, where regions of intense chemiluminescence have been observed in experiments (in C_3H_8-$5O_2$-$9N_2$ mixtures by Austin, 2003). Several issues have been ignored in our analysis, such as the increase in exchange surface provided by shear layer instability. Features associated with Kelvin-Helmotz instability have been consistently observed in Schlieren and OH fluorescence images of irregular detonations, but obviously they cannot appear in our one-dimensional simulations. When tackling much more demanding multi-dimensional calculations, however, our examples clearly suggest that the level of detail required in modeling mass and thermal transport effects should increase with the effective activation energy of the reacting mixture under study.

References

Austin, J. M. 2003 The role of instability in gaseous detonations. Ph.D. thesis, California Institute of Technology, Pasadena, CA.

Austin, J. M., Pintgen, F. & Shepherd, J. E. 2004 Reaction zones in highly unstable detonations. To be published in the Proceedings of the 30th International Symposium on Combustion, to be held July 25-30, Chicago, IL.

Clarke, J. F. 1983 On the changes in structure of steady plane flames as their speed increases. *Combust. Flame* **15**, 125–138.

Clarke, J. F. 1989 Fast flames, waves and detonation. *Prog. Energy Combust. Sci.* **15**, 241–271.

Deiterding, R. 2003 Parallel adaptive simulation of multi-dimensional detonation structures. Ph.D. thesis, der Brandenburgischen Technischen Universität Cottbus.

Giovangigli, V. 1991 Convergent iterative methods for multicomponent diffusion. *Impact Comput. Sci. Eng.* **3**, 244–276.

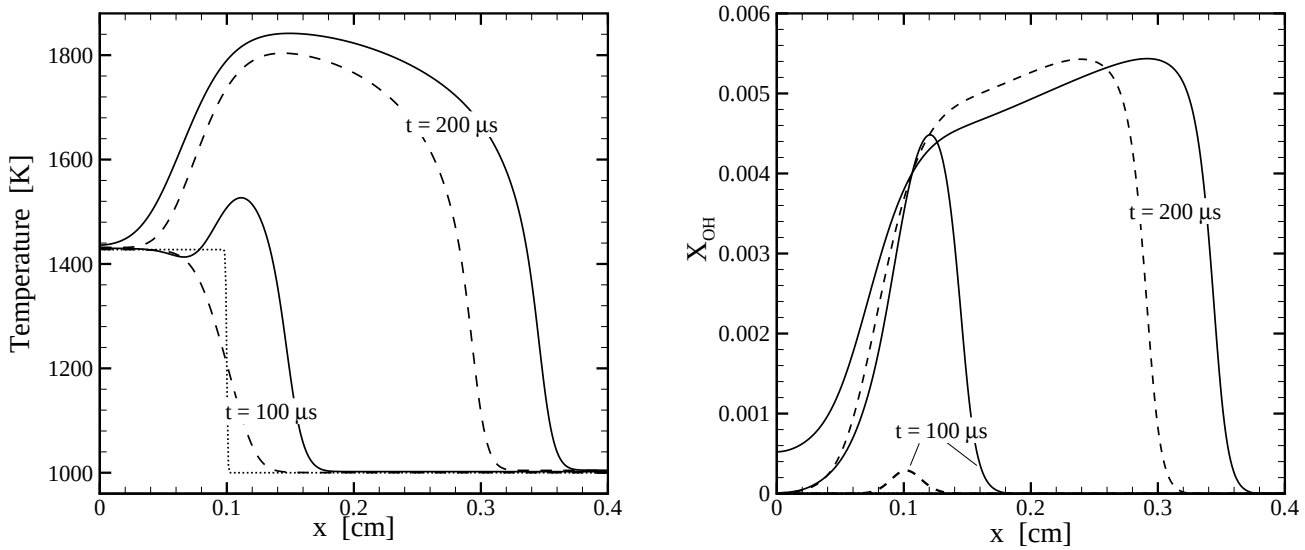

(a) (b)

Figure 5: Temperature and OH concentration for temporal development of a diffusion layer in $2H_2$-O_2-$11N_2$. Solid line: hot stream with equilibrium product composition. Dashed line: hot stream is replaced by N_2 at the same temperature. Dotted line: initial conditions.

Kee, R. J., Coltrin, M. E. & Glarborg, P. 2003 *Chemically reacting flow: theory and practice*. *Cambridge Texts in Applied Mathematics* . Wiley-Interscience.

Kee, R. J., Rupley, F. M. & Miller, J. A. 1986 A Fortran computer package for the evaluation of gas-phase multicomponent transport properties. *Tech. Rep.* SAND86-8246. Sandia National Laboratories.

Kee, R. J., Rupley, F. M. & Miller, J. A. 1987 The CHEMKIN thermodynamic data base. *Tech. Rep.* SAND87-8215. Sandia National Laboratories.

Kee, R. J., Rupley, F. M. & Miller, J. A. 1989 CHEMKIN-II: A Fortran chemical kinetics package for the analysis of gas-phase chemical kinetics. *Tech. Rep.* SAND89-8009. Sandia National Laboratories.

Knikker, R., Dauptain, A., Cuenot, B. & Poinsot, T. 2003 Comparison of computational methodologies for ignition of diffusion layers. *Combust. Sci. Technol.* **175**, 1783–1806.

Miller, J. A. & Bowman, C. T. 1989 Mechanism and modeling of nitrogen chemistry in combustion. *Prog. Energy Combust. Sci.* **15**, 287–338.

Pintgen, F., Eckett, C. A., Austin, J. M. & Shepherd, J. E. 2003 Direct observations of reaction zone structure in propagating detonations. *Combust. Flame* **133**, 211–129.

Shepherd, J. E. 1986 Chemical kinetics of hydrogen–air–diluent detonations. *Prog. Astronaut. Aeronaut.* **106**, 263–293.

Singh, S., Lieberman, D. & Shepherd, J. E. 2003 Combustion behind shock waves. In *Western States Section*. The Combustion Institute, paper 03F-29.

Smith, G. P., Golden, D. M., Frenklach, M., Moriarty, N. W., Eiteneer, B., Goldenberg, M., Bowman, C. T., Hanson, R. K., Song, S., W. C. Gardiner, J., Lissianski, V. & Qin, Z. 1995 *GRI-Mech 3.0*. `http://www.me.berkeley.edu/gri_mech/`.

Ul'yanitskii, V. Y. 1981 *Fizika Goreniya i Vzyva* **17**, 227.